

## The Fusion Core Complex of the *Peste des Petits Ruminants* Virus Is a Six-Helix Bundle Assembly<sup>†</sup>

Abdur Rahaman,<sup>‡</sup> N. Srinivasan,<sup>§</sup> N. Shamala,<sup>||</sup> and M. S. Shaila<sup>\*‡</sup>

Department of Microbiology and Cell Biology, Molecular Biophysics Unit, and Department of Physics,  
Indian Institute of Science, Bangalore 560012, India

Received September 16, 2002; Revised Manuscript Received December 3, 2002

**ABSTRACT:** We describe the properties of the two heptad repeats (HR1 and HR2) of the *Peste des petits ruminants* virus (PPRV) fusion protein (F) to obtain insights into the mechanism by which these repeats influence PPRV-mediated cell fusion. Both HR1 and HR2 inhibit PPRV-mediated syncytia formation in Vero cells in vitro. Of these, HR2 was found to be more effective than HR1. We studied the mechanism of fusion inhibition by these two repeats by using various biophysical and biochemical methods either separately or together. CD spectral analysis of these repeats revealed that the  $\alpha$ -helical content of HR1 and HR2 when used together is higher than that of their simulated spectrum in the mixture, suggesting the formation of a highly structured complex by these repeats. Protease protection assays confirmed that such a complex is highly stable. Electrospray mass spectrometry of protease-digested products of the HR1–HR2 complex showed protection of fragments corresponding to both HR1 and HR2 sequences involved in complex formation. By employing size-exclusion chromatography and chemical cross-linking experiments, we show that three units each of HR1 and HR2 form a complex in which HR1 is a trimer and HR2 is a monomer. Homology-based three-dimensional modeling of this complex showed that HR1 and HR2 together form a six-helix and trimeric coiled-coil bundle. In this model, the HR1 trimer forms the core whereas HR2, while interacting with HR1 in an antiparallel orientation, forms a two-stranded coiled-coil structure and lies at the periphery of the structure. These results are discussed in the context of a common fusion mechanism among paramyxoviruses.

*Peste des petits ruminants* (PPR)<sup>1</sup> or “goat plague” is caused by the PPR virus (Paramyxoviridae; morbillivirus), an enveloped, negative sense single-stranded RNA virus. The PPRV genome encodes six structural proteins, namely, nucleocapsid protein (N), phosphoprotein (P), matrix protein (M), fusion protein (F), hemagglutinin-neuraminidase protein (HN), and large protein (L). N protein encapsidates the genomic RNA to form the N–RNA template to facilitate replication and transcription by the L–P polymerase complex. M is a matrix protein around which the envelope is

assembled. F and HN are two surface glycoproteins which enable the entry of the virus into the host cell; H recognizes the host cell receptor, whereas F mediates the fusion of host and viral envelopes. The PPRV F protein does not require the HN protein to bring about biological fusion, a property shown by the paramyxovirus SV5, while the other members in the Paramyxoviridae family require the fusion promotion function mediated by HN or H protein (1–13). The F protein-mediated fusion process has been extensively investigated in other paramyxoviruses (14). In general, it is synthesized as a precursor (F<sub>0</sub>) which is cleaved by the host machinery into two fragments, F<sub>1</sub> and F<sub>2</sub>, which are linked by a disulfide bond. Of these, F<sub>1</sub> forms a membrane-anchoring subunit (15–18). This subunit has several conserved motifs among paramyxoviruses of which four are well studied: (1) a fusion peptide (FP) at the newly generated N-terminus, (2) heptad repeat 1 (HR1), (3) another heptad repeat (HR2), and (4) the transmembrane (TM) domain (19–25). Of these conserved motifs, FP, HR1, and HR2 mediate fusion of the viral envelope and host cell membrane. In this process, FP is inserted into the host cell membrane whereas two heptad repeats interact with each other and bring the host cell membrane and viral envelope into proximity which in turn results in fusion. Such fusion has been shown to be affected by exogenously added HR1 and/or HR2 motifs from F proteins of various paramyxoviruses (26–34). Recent studies on the fusion processes of envelope viruses have led to the identification of a common core structure formed by HR1

<sup>†</sup> This research was partly supported by the Council of Scientific and Industrial Research, Government of India, New Delhi. The infrastructural facilities provided by the Department of Biotechnology, Government of India, under the program support are acknowledged. A.R. was a senior research fellow of the University Grant Commission, Government of India, and N. Srinivasan is supported by the Senior Research Fellowship program for Biomedical Research by the Wellcome Trust (London, U.K.).

<sup>\*</sup> To whom correspondence should be addressed: Department of Microbiology and Cell Biology, Indian Institute of Science, Bangalore 560012, India. Phone: 91-80-3600139/3942702. Fax: 91-80-3602697. E-mail: shaila@mcbl.iisc.ernet.in.

<sup>‡</sup> Department of Microbiology and Cell Biology.

<sup>§</sup> Molecular Biophysics Unit.

<sup>||</sup> Department of Physics.

<sup>1</sup> Abbreviations: PPRV, *peste des petits ruminants* virus; HR1, heptad repeat region 1; HR2, heptad repeat region 2; SV5, simian virus 5; FP, fusion peptide; SEC, size-exclusion chromatography; CD, circular dichroism; DLS, dynamic light scattering; MV, measles virus; RSV, respiratory syncytial virus; NDV, Newcastle disease virus; SV, Sendai virus; HIV, human immunodeficiency virus; SIV, simian immunodeficiency virus.

and which has helped in exploring inhibitors of viral fusion proteins, a promising new means of targeting a wide group of viruses (25, 35–38).

Here we report the biochemical and biophysical properties of recombinant HR1 and HR2 motifs of PPRV F and studies on their biological functions. We also propose a structure for the fusion core (HR1–HR2 complex) of PPRV F. This structure is based on sequence homology of PPRV F with that of the SV5 fusion core, the crystal structure of which has recently been determined (39). These results are discussed in light of common steps in virus-host cell fusion among paramyxoviruses.

## MATERIALS

C41 and C43 strains derived from the BL21(DE3) version of *Escherichia coli* were gifts from J. E. Walker (40). The vaccine strain of PPRV (Nigeria 75/1) was obtained from A. Diallo (CIRAD-EMVT, France). *E. coli* DH5 $\alpha$  was used for maintenance of plasmids BlueScript KS+ (Stratagene), pRSET A, and pGEX 4T-1 (Invitrogen). The pSS97-2 plasmid containing the full-length PPRV F gene in pC-MX.PL1 was derived from a cDNA clone (pADPPRF) of the PPRV F Nigerian 75/1 strain lacking 300 nucleotides from the 5'-untranslated region (1, 41). Vero cells from African green monkey (*Cercopithecus aethiops*) kidney cells were from ATCC. These cells were maintained on DMEM containing 5% FCS (GIBCO BRL). The protease inhibitor cocktail was from Sigma Co. Ni-NTA agarose was from Qiagen and Sephadex G75 from Amersham-Pharmacia.

## METHODS

**Preparation of the Virus Stock.** Monolayers of Vero cells were trypsinized at 37 °C for 1 min using 0.1% trypsin and subcultured in DMEM supplemented with 5% FCS. Cells 24 h after subculturing (~70% confluent) were infected with 1–2 mL of diluted PPRV (approximately 0.1–1 pfu/cell) and incubated at 37 °C for 3–4 days until a 70–80% cytopathic effect (CPE) was seen. The bottles were frozen and thawed thrice, and the medium was collected as a virus stock for further use. Virus titer was measured by end point dilution, and TCID<sub>50</sub> was calculated by employing the formula of Reed and Muench (42).

**Cloning of HR1 and HR2 of PPRV F.** HR1 and HR2 were amplified using pSS97-2 DNA as a template and the appropriate primers [forward, 5' CAA GGA TCC ATC GAA GGT CGT (382) ACT GCC GGA GTC GCA C 3' for HR1 and 5' CAA GGA TCC ATC GAA GGT CGT (1300) CCA GAT TCT GTA TAC C 3' for HR2; reverse, 5' AAT GG GTC GAC (570) TCA TGA CAT TCT ATG AAC AG 3' for HR1 and 5' GGA TT GTC GAC TA (1452) TTT AAC AGT CTT CAG TAT C 3' for HR2]. Nucleotide positions of all the primers on the F gene are indicated in parentheses. In both the cases, the forward primer had a *Bam*HI restriction site followed by a factor Xa cleavage site and the reverse primer had a stop codon followed by a *Sal*I restriction site. These modifications were included to remove additional amino acids from the expressed proteins.

The PCR products were cloned in the *Sma*I site of pBS KS+. The inserts from recombinants were released using *Bam*HI and *Sal*I and subcloned into similar restriction sites

of pGEX 4T-1. The inserts were finally subcloned into *Bam*HI- and *Xho*I-digested pRSET-A.

**Expression of HR1 and HR2 as His-Tagged Proteins.** *E. coli* BL21(DE3) C41 and C43 strains were transformed with plasmids carrying HR1 and HR2, respectively. After overnight growth at 37 °C, few colonies were inoculated into LB containing 100  $\mu$ g/mL ampicillin and induced with 0.4 mM isopropyl thiogalactopyranoside (IPTG) at an OD<sub>600</sub> of 0.6 and grown for an additional 5 h. The cells were harvested and lysed by sonication in MCAC buffer [500 mM NaCl in 20 mM Tris-HCl (pH 8)] supplemented with 2 mM PMSF and the protease inhibitor cocktail. The lysates were centrifuged, and supernatant was mixed with Ni-NTA agarose. The resin was washed with 100 bed volumes of MCAC buffer containing 50 mM imidazole in the case of HR1 and 25 mM imidazole in the case of HR2. Proteins were eluted with 500 mM imidazole in MCAC supplemented with the protease inhibitor cocktail. Eluted samples of purified proteins were detected by Coomassie staining of 15% SDS–polyacrylamide gels.

**Cleavage of HR1 and HR2 Peptides from His-Tagged Fusion Proteins.** The purified proteins were dialyzed against factor Xa cleavage buffer [20 mM Tris-HCl (pH 8.0), 100 mM NaCl, and 2 mM CaCl<sub>2</sub>] and cleaved with factor Xa [final concentration of 1% (w/w)] at 23 °C for 5 h. Ni-NTA agarose was added to the cleavage products to eliminate the histidine tags as well as uncleaved products. The unbound fractions containing cleaved peptides were collected, and factor Xa was inactivated by adding EDTA (final concentration of 2 mM). The cleaved products were resolved on a 15% SDS–polyacrylamide gel and detected with silver staining. Both the peptides were purified to near homogeneity on a C18 semipreparative column by reverse-phase HPLC (Hewlett-Packard, series 1090 system) using a linear gradient of acetonitrile.

**Mass Spectroscopic Analysis.** Both HR1 and HR2 obtained by reverse-phase chromatography were analyzed by electrospray ionization (ESI) mass spectroscopy (Hewlett-Packard 1100 system with a quadrupole mass detector).

**Circular Dichroism (CD) Spectroscopy.** HR1 and HR2, purified using C18 columns, were lyophilized and resuspended in phosphate-buffered saline (PBS) at 0.1 mg/mL and analyzed in a spectropolarimeter (JASCO J-715) at room temperature. The CD spectrum was measured in a cuvette with a path length of 2 mm, with a bandwidth of 0.5 nm and a scan speed of 50 nm/s. The buffer spectrum was subtracted from the protein spectrum. An average of four independent measurements were used to calculate the molar residue ellipticity,  $[\theta]_{MRW}$ , using the formula

$$[\theta]_{MRW} = (100M_r\theta)/(clN_A)$$

where  $[\theta]$  is mean residue molar ellipticity in degrees per inverse square centimeter per decimole,  $\theta$  is the experimental ellipticity in millidegrees,  $M_r$  is the molecular mass of the protein in daltons,  $c$  is the protein concentration in milligrams per milliliter,  $l$  is the cuvette path length in centimeters, and  $N_A$  is the number of residues in the protein. The percentage helicity was estimated as follows (43, 44):

$$\% \text{ helicity} = [([\theta]_{222} - {}^0[\theta]_{222}) / ({}^{100}[\theta]_{222} - {}^0[\theta]_{222})] \times 100$$



FIGURE 1: Structure of PPRV F. (a) Schematic diagram of the protein showing F<sub>1</sub> and F<sub>2</sub> subunits connected by a disulfide linkage (••). Also shown are the positions of the fusion peptide (FP), HR1, HR2, and the transmembrane domain (TM) of the F<sub>1</sub> subunit. (b) Amino acid sequences of HR1 and HR2 used in this study. AR denotes the additional 17 vector-encoded residues resulting from cleavage by factor Xa after an arginine residue on the tag instead of the site incorporated preceding the N-termini of both peptides.

where  $[\theta]_{222}$  is the experimentally observed absolute mean residue ellipticity at 222 nm and values for  $^{100}[\theta]_{222}$  and  $^0[\theta]_{222}$ , corresponding to 100 and 0% helix content at 222 nm, respectively, were estimated to be 2000 and 32 000 deg cm<sup>2</sup> dmol<sup>-1</sup>, respectively (44, 45).

**Size-Exclusion Chromatography (SEC).** A Sephadex G75 column (45 cm × 2.22 cm<sup>2</sup>, bed volume of 100 mL) was equilibrated with PBS and calibrated using standard protein molecular mass markers. One milligram each of histidine-tagged HR1 or HR2 was resuspended in 1 mL of PBS and fractionated separately or together (by incubating an equimolar mixture of HR1 and HR2 at room temperature for 2 h) on the same column, and the elution profile was monitored by estimating the protein content by measuring the absorbance at 280 nm. The proteins were then identified by using SDS-polyacrylamide gels and silver staining.

**Chemical Cross-Linking.** Approximately 10 μg of histidine-tagged HR1 peptide was cross-linked using dithiobis(succinimidylpropionate) (final concentration of 1 mM) for different time intervals from 1 to 6 h at 25 °C. The reaction was stopped by adding 200 mM glycine, and the products were mixed with SDS-PAGE loading dye (without β-mercaptoethanol), electrophoresed on a 15% SDS-polyacrylamide gel, and detected by silver staining.

**Limited Proteolysis of HRs.** Equimolar amounts of histidine-tagged HR1 and HR2 in PBS were incubated for 2 h at room temperature and cleaved with proteinase K [5% (w/w) of each peptide] for 3 h. In control experiments, HR1 and HR2 peptides were incubated separately with proteinase K. The reaction was stopped by adding PMSF (final concentration of 5 mM); the samples were subjected to SDS-PAGE analysis on a 15% Tricine gel, and the proteins were visualized by silver staining. The digested products of the HR1/HR2 mixture were also subjected to ES-MS after passing through the C18 reverse-phase columns using acetonitrile as a solvent.

**Fusion Inhibition Assay.** Vero cells were plated in 35 mm wide tissue culture dishes at a density of 1 × 10<sup>6</sup> cells/2 mL of DMEM supplemented with 5% FCS. These cells at 70% confluence were infected with PPRV Nigerian 75/1 (1–2 TCID<sub>50</sub>/cell) for 1 h at room temperature and incubated with different concentrations of either HR1 or HR2 in DMEM (supplemented with 3% FCS) at 37 °C for 48 h. Following infection, the cells were washed with PBS, fixed with a methanol/acetic acid (95:5) mixture for 20 min at –20 °C, washed again with PBS, stained with Giemsa (diluted 10 times in PBS) for 30 min at room temperature, and observed under a light microscope. The extent of fusion was ascertained by visualizing in 10 different fields for the presence of syncytia. The percent syncytia obtained by using the

peptide inhibitors was calculated as given below:

$$\frac{\text{number of syncytia observed in the presence of HR1 or HR2}}{\text{total number of syncytia observed in the control experiment}} \times 100$$

**Secondary Structure and Coiled-Coil Predictions.** Both HR1 and HR2 sequences of PPRV F were subjected to secondary structure prediction using the PHD program (46, 47) and coiled-coil prediction using the multicoil program (48) to examine the potential of these two motifs to form coiled-coil structure.

**Modeling.** Sequence analysis by clustalW (49) showed a high degree similarity of the HR1 (~73% similar and 36% identical) and HR2 (~65% similar and 27% identical) regions between the PPRV F protein and that of SV5, the crystal structure of which has recently been reported (39). This high degree of sequence similarity suggested a similar fold between these two proteins and was further confirmed by comparing the structural features which shows very high similarity among hydrophobic residues involved in interaction between the subunits. A structural model was built using the COMPOSER suite programs incorporated in SYBYL (50–52). Initially, the HR1–HR2 heterodimer was modeled and the energy-minimized model of this heterodimer was superimposed on the template trimeric structure to achieve the trimeric form. The trimer was also subjected to energy minimization to obtain the final structure without having any short contacts or bad bond angles or bond lengths. Energy minimization was carried out using the AMBER force field also incorporated in SYBYL (53). During the initial cycles of energy minimization, the backbone was kept rigid, allowing all the side chains to move. Subsequently, all the atoms in the structure were allowed to move until all the short contacts were relieved and bad geometries rectified. The ribbon diagram of the model was generated using SETOR (54).

## RESULTS

**Recombinant HR1 and HR2 Motifs of PPRV F.** HR1 and HR2 of PPRV F (Figure 1) were identified by comparing the F protein sequences of PPRV with those from SV5 and MV. Sequences corresponding to PPRV F protein residues 128–190 (HR1) and 434–484 (HR2) were amplified, cloned, and expressed using the pRSET vector in *E. coli* C41 and C43, respectively. The HR1 peptide contains seven additional amino acids derived from the fusion peptide along with entire HR1 region, whereas recombinant HR2 has the entire HR2 region with additional residues of F at its N-terminus. Figure 2 shows the expression profile of these

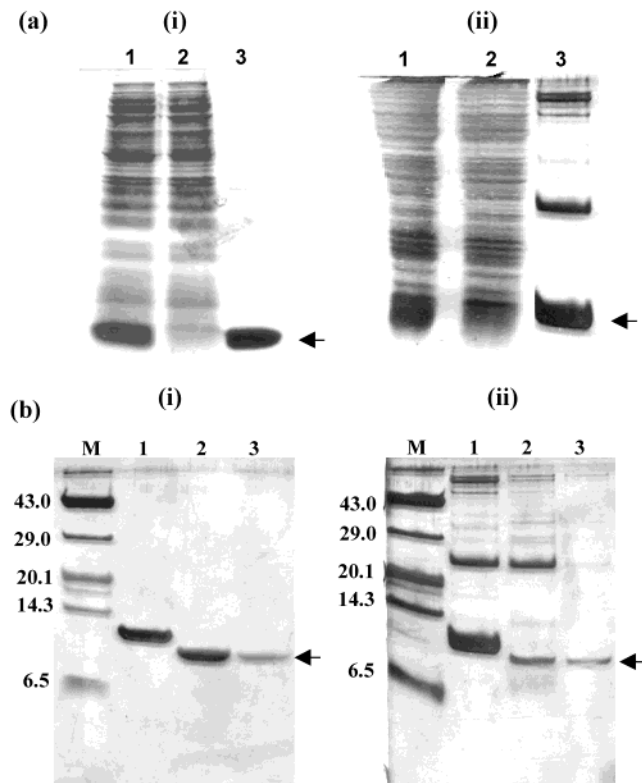


FIGURE 2: (a) SDS-PAGE of recombinant HR1 (i) and HR2 (ii): lane 1, crude cell lysate; lane 2, unbound fraction of the Ni-NTA agarose column; and lane 3, purified protein. (b) Tricine (15%) gel showing the factor Xa cleavage pattern of HR1 (i) and HR2 (ii): M, protein markers (kilodaltons); lane 1, purified protein without factor Xa; lane 2, purified protein with factor Xa; and lane 3, cleaved product after passing through a Ni-NTA agarose column. Arrows indicate the respective peptides. Additional high-molecular mass bands in the nickel affinity-purified fraction of HR2 as in lane 3 of part ii of panel a may arise from *E. coli* BL21(DE3) cells used for expression which are eliminated from the cleaved peptide after passing through Ni-NTA agarose as in lane 3 of part ii of panel b.

histidine-tagged recombinant proteins and their cleavage by factor Xa after their purification using an Ni-NTA agarose column. Mass spectroscopy of the cleavage products revealed the presence of an additional 17 vector-encoded amino acids at the N-terminus. These cleavage products were purified by HPLC and used in the experiments described below.

**Effect of HR1 and HR2 on PPRV-Mediated Cell-Cell Fusion.** Vero cells, infected with PPRV, were incubated with HR1 or HR2 and assayed for formation of syncytia, an indication of virus-induced cell-cell fusion. Addition of both HR1 and HR2 resulted in a significant decrease in the number of syncytia as compared to the number in a sample to which no peptide was added (Figure 3). HR1 ( $3 \mu\text{M}$ ) and HR2 ( $1 \mu\text{M}$ ) resulted in a 50% reduction in the number of syncytia. At  $\sim 6$  and  $\sim 3 \mu\text{M}$ , respectively, both HR1 and HR2 completely abolished syncytia formation. These results indicate that HR2 is a more potent inhibitor of PPRV-induced cell-cell fusion than HR1.

**HR1 and HR2 Interact with Each Other and Form a Protease-Resistant Complex.** In paramyxovirus such as SV5 and RSV, HR1 and HR2 of F have been reported to interact with each other and form a six-membered fusion core. Therefore, the possibility of such interaction in PPRV was studied. The results of CD spectroscopy (Figure 4) suggested

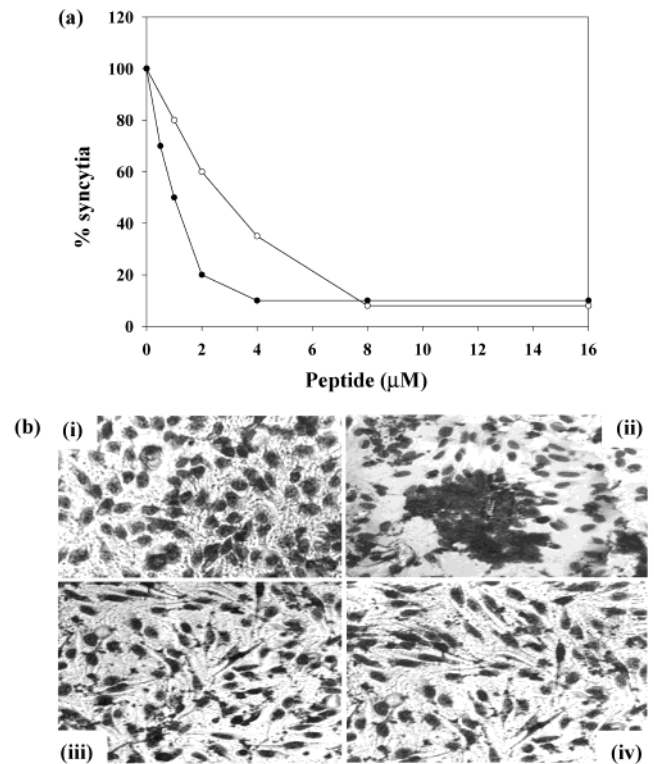


FIGURE 3: Fusion inhibition activity of HR1 and HR2. Vero cells infected with PPRV Nigeria 75/1 were incubated with different concentrations of either HR1 or HR2 for 48 h. (a) Graph showing percent syncytia formation at different concentrations of HR1 (○) and HR2 (●). (b) Uninfected control Vero cells (i), Vero cells infected with virus showing syncytia formation (ii), and virus-infected Vero cells treated with either  $6 \mu\text{M}$  HR1 (iii) or  $3 \mu\text{M}$  HR2 (iv). At these concentrations, both HR1 and HR2 completely inhibit syncytia formation.

that while HR1 formed  $\alpha$ -helices ( $\sim 52\%$   $\alpha$ -helix content), most of HR2 was a random coil (negligible  $\alpha$ -helix content). When both HR1 and HR2 were used, there was a significant increase in the amount of secondary structure (mainly  $\alpha$ -helices). The observed amount of secondary structure of the mixture ( $\sim 60\%$   $\alpha$ -helices) is 2 times greater than the mean of their individual  $\alpha$ -helix contents ( $\sim 28\%$ ). Though the percent  $\alpha$ -helix content of this complex in PPRV (60%) is less than those observed in SV5 (82%), RSV (86%), and NDV ( $>80\%$ ), this could be attributed to the additional vector-encoded residues in both peptides of PPRV, as they would be expected to remain in the random-coil conformation. These results suggest that HR1 and HR2 of PPRV F as in other paramyxoviruses (RSV, NDV, and SV5) interact with each other. The HR1-HR2 interaction was also confirmed by subjecting the mixture of HR1 and HR2 to proteinase K digestion. As shown in Figure 5a, both HR1 and HR2 were completely digested when used separately; however, a mixture of HR1 and HR2 was resistant to digestion by the enzyme. Two of these proteinase K-resistant fragments correspond to molecular masses of 5289 and 5042 Da, respectively (Figure 5b). When these molecular masses are extrapolated to HR1 and HR2 sequences, the larger fragment (MW = 5289 Da) corresponds to HR2 lacking two C-terminal amino acids (MW = ca. 5290 Da), whereas the smaller fragment (MW = 5042 Da) corresponds to HR1 without ten N-terminal and eight C-terminal amino acids (MW = ca. 5047 Da). It may be noted that histidine tags of

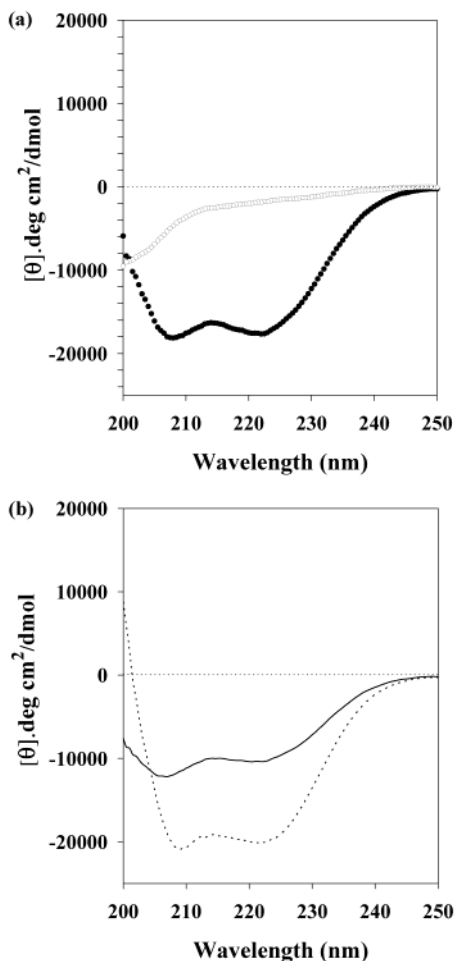


FIGURE 4: Interaction of HR1 and HR2. (a) CD spectra of 10  $\mu$ M HR1 ( $\bullet$ ) and 10  $\mu$ M HR2 ( $\circ$ ). (b) CD spectrum of a mixture of 10  $\mu$ M HR1 and 10  $\mu$ M HR2 ( $\cdots$ ) along with the simulated spectrum of noninteracting HR1 and HR2 ( $-$ ). The enhanced negative ellipticity in the CD spectrum of the mixture as compared to that in the simulated spectrum signifies a specific interaction between HR1 and HR2.

HR1 and HR2 were completely digested, leaving only specific stretches of amino acids that participate in the HR1–HR2 interaction. Since no protected fragment was detected when HR1 or HR2 was used separately, we conclude that protection of HR1 and HR2 in the mixed solution is due to the formation of the HR1–HR2 complex.

**Analysis of HR1 and HR2 Peptides and Their Complex.** To understand the nature of the HR1–HR2 complex, size-exclusion chromatography was performed. Figure 6a shows that the complex eluted at a position corresponding to a molecular mass of approximately 63 kDa, which is thrice the sum of the molecular masses of HR1 and HR2, suggesting that the complex contains three molecules each of HR1 and HR2. To study whether HR1 and HR2 are capable of forming oligomers by themselves, size-exclusion chromatography (SEC) and chemical cross-linking experiments were carried out. SEC showed that HR1 eluted at a molecular mass corresponding to 34 kDa (Figure 6b), whereas HR2 eluted at 10 kDa (Figure 6c). Since the calculated molecular mass of HR1 is 11 kDa, these results indicate that HR1 exists as a trimer. The occurrence of such trimers was also confirmed by chemical cross-linking. As shown in Figure 7, in addition to the monomeric form, cross-

linked HR1 was detected as dimers as well as trimers. With an increase in the duration of cross-linking, an increase in the amounts of trimers was observed. Since cross-linked products higher than trimers were not observed, these results led us to conclude that HR1 occurs only as a trimer. We did not perform cross-linking studies with HR2 because size-exclusion chromatography indicated that it is only a monomer. Taken together, these results indicate that the HR1–HR2 complex is a trimer of dimers, the dimer being one molecule each of HR1 and HR2.

**Structural Features of the PPRV F Fusion Core.** Secondary structure prediction using PHD (46, 47) showed the  $\alpha$ -helical nature of both HRs. The multicoil program (48) predicted the coiled-coil structure, and the sequence of HRs was modeled using the triple-stranded coiled-coil structure of the SV5 F fusion core as the template. The levels of sequence similarity in the HR1 and HR2 regions of PPRV F were  $\sim 73$  and  $\sim 69\%$ , respectively, with the corresponding regions of the template structure. The overall structure showed a six-helical triple-stranded coiled coil (Figure 8) in which the inner side of the core is formed by the HR1 trimer and HR2 forms the outer layer by interaction with HR1 in an antiparallel manner. Interestingly, HR2 of one heterodimer interacts with HR1 of the adjacent heterodimer and further stabilizes the trimeric structure. In this model, conserved hydrophobic residues are involved in both HR1–HR1 and HR1–HR2 interactions. By sequence analysis of HR1 in F proteins from various paramyxoviruses, Joshi et al. (32) observed that in addition to positions a and d in the a–g heptad repeat, the residues in positions e and g are also conserved (primarily as hydrophobic residues). Among the 11 residues conserved in the HR1 and HR2 regions in the paramyxoviruses, five residues, namely, A123, I137, T147, L453, and L474, in the template structure form part of the HR1–HR1 or HR1–HR2 buried interface. The corresponding residues in PPRV F are the same as in the template structure except T147 of the crystal structure is replaced with serine. In the crystal structure, T147 forms a hydrogen bond network with S470, N148, and D491 in SV5. In the model derived here, serine is also involved in a similar network, resulting in a similar structure in these two repeat regions. In SV5, Q169 and N173 form hydrogen bonds with backbone residues L447 and I449. These amino acids are conserved or conservatively substituted in PPRV F and are responsible for the transition of the extended chain to  $\alpha$ -helical structure in HR2. In addition, few other residues important for coiled-coil core formation are either unchanged (e.g., V165 and V168) or replaced (e.g., H171 of SV5 F is replaced with tyrosine in PPRV F). It may be noted that Baker et al. (39) have suggested that H171 in their model can be replaced with tyrosine (39). Conservation of all these residues signifies that PPRV F has a core structure similar to SV5 and is unstructured in the region preceding the C-terminal  $\alpha$ -helix of HR2.

## DISCUSSION

Fusion of the viral envelope with the host membrane is an important step in infection, and hence, drugs affecting this process are believed to be most effective (36–38). As mentioned before, F proteins of paramyxoviruses are important components of the fusion process and are being studied intensively. We studied the effect of exogenously

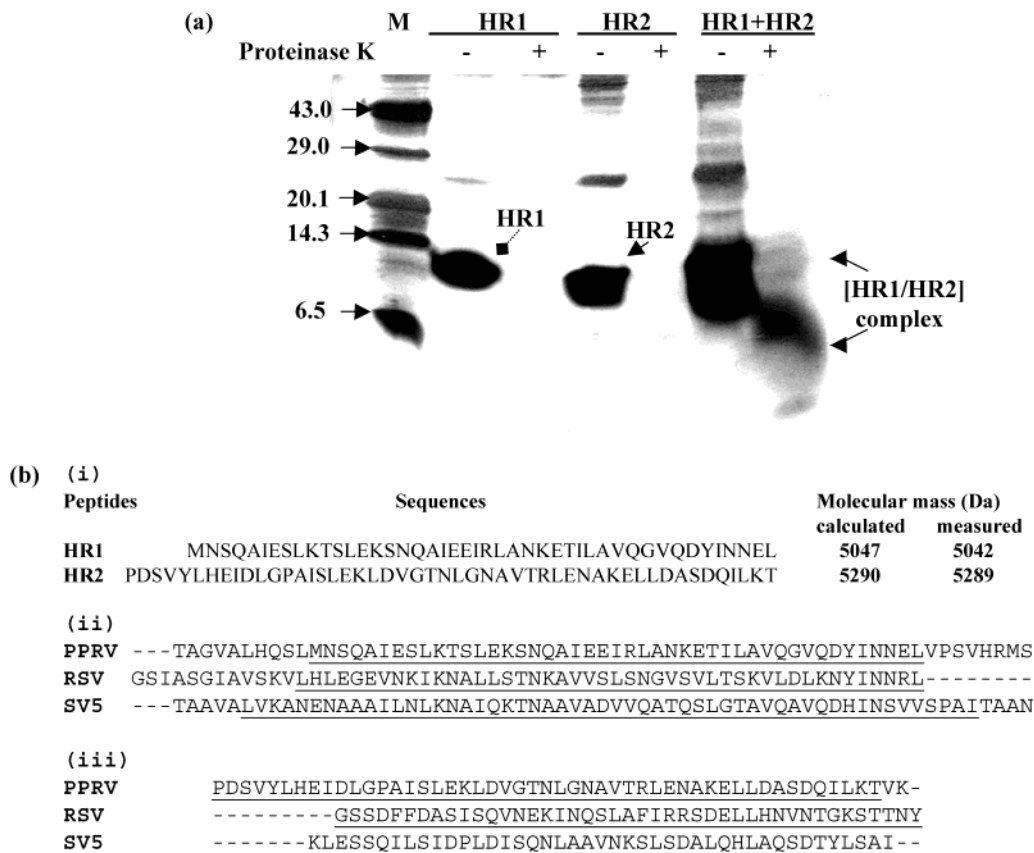


FIGURE 5: Protection of the HR1–HR2 complex from proteolytic cleavage. (a) Tricine (15%) gel showing HR1, HR2, and their complex incubated in the presence (+) or absence (–) of proteinase K as indicated at the top. Lane M contained protein markers (kilodaltons). The mixture of HR1 and HR2 was incubated at room temperature prior to proteinase K treatment. (b) Amino acid sequences of HR1 and HR2 peptides identified by ES-MS after the proteinase K-digested products of the HR1–HR2 complex had been passed through the reverse-phase HPLC system (i) and alignments of amino acid sequences of HR1 regions (ii) and HR2 regions (iii) of F proteins from PPRV, SV5, and HRSV in which the sequences protected from protease digestion are underlined.

added HR1 and HR2 motifs on the PPRV-mediated fusion of Vero cells. While both HR1 and HR2 inhibit fusion, HR2 was found to be more potent than HR1; 50% inhibition was observed with 1  $\mu$ M HR2 or 3  $\mu$ M HR1. A similar difference has also been reported in SV5 (32). The molar differences in the requirement for fusion inhibition were attributed to the differences in the steps in which HR1 and HR2 are involved; HR2 affects lipid mixing and HR1 contents mixing (32).

Our observation that HR1 exists as a trimer needs to be viewed in the apparent differences in molar requirements for these two peptides. We suggest that the trimeric form of PPRV HR1 may be either intrinsic or a prerequisite for fusion inhibition. Recent studies on sendai virus (SV) support our hypothesis that SV HR1 occurs predominantly as a monomer and was found to be effective in fusion inhibition at only very high concentrations (33). It may also be likely that in SV, at a very high concentration, a few HR1 trimers are formed.

With regard to the requirement of HN/H for F-mediated fusion, paramyxoviruses fall into two categories: those which require HN/H and those which are HN/H-independent. In PPRV and SV5, F-mediated fusion can occur without the requirement of HN (1, 2) and HR1 in these viruses can cause fusion inhibition (ref 32 and this study). On the other hand in viruses such as MV, SV, and NDV, HN/H is required for fusion (7, 9, 55). In the latter group, HR1 cannot inhibit F-mediated fusion (33, 56, 57). It has been suggested that

in viruses such as MV, SV, and NDV, HN/H prevents the interaction of HR1 with F and affects HR1-induced fusion inhibition (57). Therefore, the differences in the intrinsic ability of HR1 in causing fusion inhibition correlate with the HN dependence or independence of F-mediated fusion among these paramyxoviruses.

Paramyxoviruses also fall into two categories on the basis of amino acid requirements of HR2 for causing fusion inhibition. In NDV, a 20-amino acid peptide (FZ20) in the C-terminus of HR2 causes fusion inhibition whereas additional amino acids in its N-terminus are required for such inhibition in MV and SV5 (31, 32, 56). In the case of PPRV also, a 20-amino acid peptide (FZ20) in the C-terminus of HR2 does not inhibit virus-mediated fusion (A. Rahaman et al., unpublished result), but the peptide in the study presented here containing the entire HR2 causes fusion inhibition. These results suggest that PPRV belongs to the category of MV and SV5. This prompted us to propose that there are common structural intermediates among PPRV, MV, and SV5 F proteins which differ from NDV F during fusion processes.

A six-helix bundle of the HR1–HR2 complex among paramyxovirus fusion cores is believed to represent the structure involved in fusion promotion or is a result of fusion promotion (25). This structure in PPRV is a trimer of the HR1–HR2 heterodimer. While HR1 is highly  $\alpha$ -helical in solution, consistent with its coiled-coil nature, HR2 is a random coil under similar conditions. This unstructured

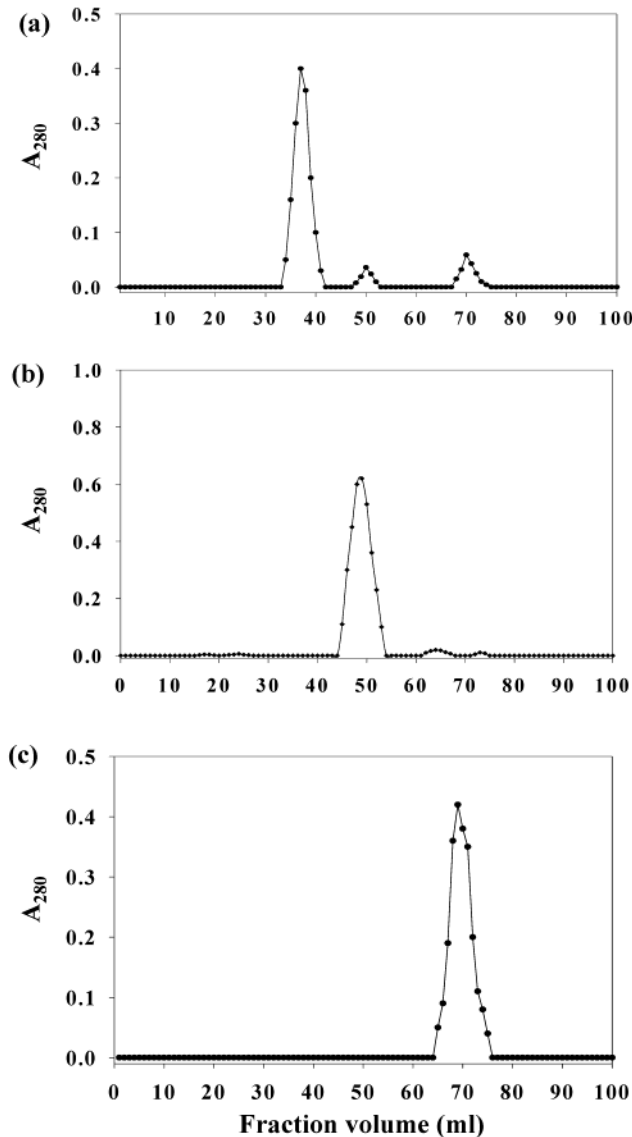


FIGURE 6: Gel filtration analysis of the HR1–HR2 complex. Ni–NTA-purified histidine-tagged HR1 or HR2 or a mixture was fractionated on the Sephadex G75 column, and  $A_{280}$  was measured for each fraction. (a) The elution profile of the mixture shows a hexameric complex. The smaller peaks represent the HR1 trimer and the HR2 monomer. (b) and (c) Elution profiles of HR1 and HR2, respectively.

conformation of HR2 is a common feature among paramyxoviruses except NDV (29, 31, 32, 38, 58, 59). A specific interaction of PPRV HR1 and HR2 peptides results in a complex with a significant change in secondary structure (mainly  $\alpha$ -helix content), suggesting that the unfolded HR2 becomes structured (mostly  $\alpha$ -helical) in the complex. Results similar to those reported in this work were obtained using HR1 and HR2 of SV5, RSV, and NDV by other investigators (32, 38, 57, 59).

The nature of the HR1–HR2 complex structure is such that it is resistant to cleavage by proteinase K (Figure 5). Mass spectroscopic analysis of the digestion products showed that the entire HR2 and most of the HR1 were protected in the complex (Figure 8). This complex therefore appears to be similar to that of RSV (59). However, this complex differs from SV5 in which only HR1 is protected from protease digestion (32). In SV5, only a small portion of HR2 when used with HR1 appears to be resistant to protease. While

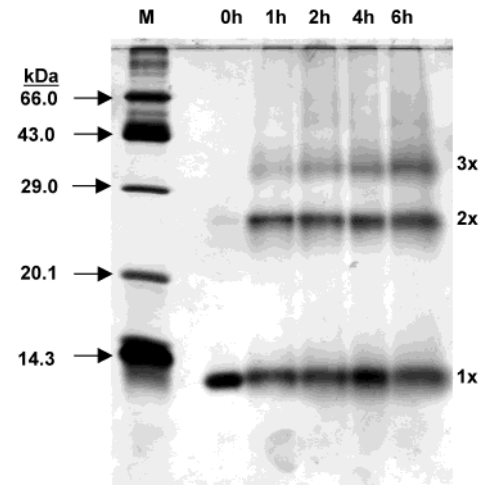


FIGURE 7: Chemical cross-linking analysis of HR1. Approximately 10  $\mu$ g of histidine-tagged HR1 was incubated with 1  $\mu$ M dithiobis-(succinimidylpropionate) (DSP) for 0–6 h at 25  $^{\circ}$ C. SDS–PAGE (15%) showing dimeric (2x) and trimeric (3x) bands along with monomers (1x) at different time intervals.

these experiments in SV5 need to be resolved further, the results suggest that despite some differences in these complexes among SV5, RSV, and PPRV, all paramyxoviruses, including NDV and PPRV, have a common fusion core structure, with varying degrees of resistance to protease (32, 57, 59).

The three-dimensional model for the PPRV F HR1–HR2 complex shows that the HR1 trimer forms the inner core and HR2 forms a heterodimer with HR1 in an antiparallel orientation, resulting in a six-helix bundle. Although there are substitutions of some amino acids between the crystal structure and modeled structure, they perform a similar structural role, resulting in a similar structure of the HR1–HR2 complex in these two viruses. The characteristics of the proposed model are consistent with our results. (a) The trimeric and highly  $\alpha$ -helical nature of the HR1 peptide indicates a triple-stranded coiled-coil structure. (b) Interaction of HR2 (monomer) with the HR1 trimer forming a hexameric complex strongly suggests a complex containing a trimer of each heterodimer. (c) The stability and the structured nature of the complex are also evident from CD spectral analysis and protease resistance of this HR1–HR2 complex. Although in the complex the orientation of HR1 and HR2 with respect to each other is not addressed, it can be extrapolated to be antiparallel from the known structures of the complexes of other paramyxoviruses, such as SV5 and RSV (39, 60, 61). A complex of this nature is common not only in the fusion proteins of paramyxoviruses but also in other enveloped viruses such as influenza virus HA protein, HIV1/SIV gp41 protein, and env proteins of retroviruses (25, 35). The crystal structures of influenza virus HA protein in its fusion active and inactive forms suggested that the stable fusion core structure either is required for fusion or is a consequence of the fusion event (62–64). Although there are differences in the requirements for influenza and paramyxoviruses for fusion initiation, Baker et al. (39) suggested similar intermediary steps in the fusion processes among these viruses (39). In influenza virus, low pH acts as trigger for a change in the conformation of HA (equivalent to F in paramyxoviruses) (65). What triggers such conformational change in the F proteins of paramyxoviruses is not clear. Recently, HN

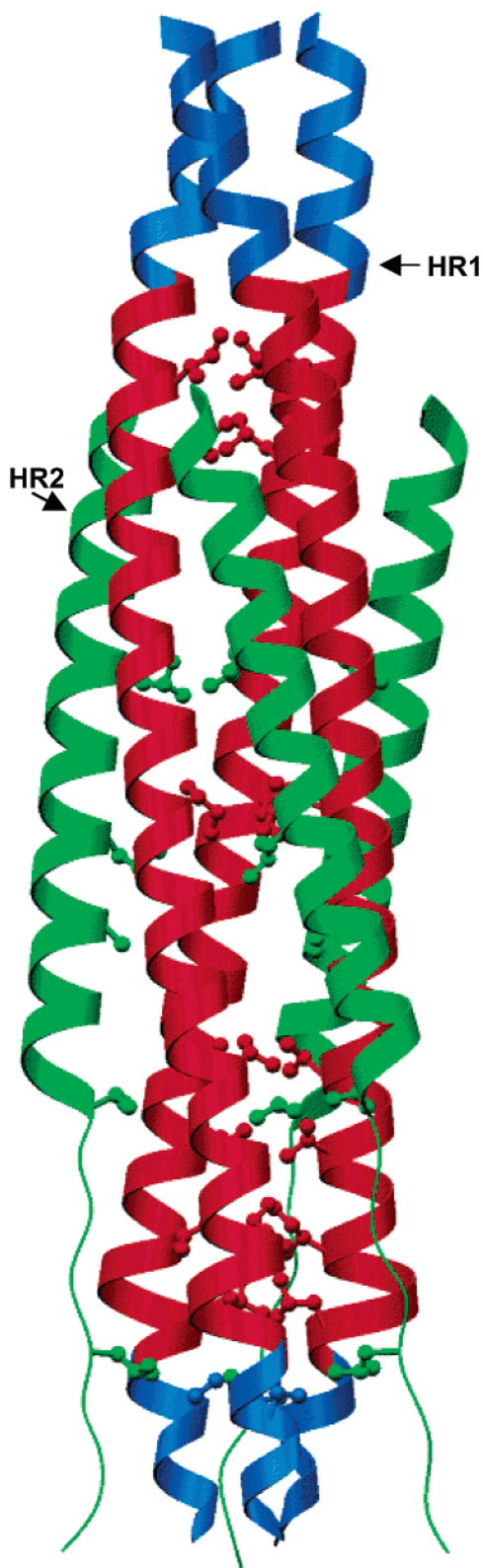


FIGURE 8: Three-dimensional model structure of the HR1–HR2 complex of PPRV F. The side chains of HR1 and HR2 involved in interactions (HR1–HR1 and HR1–HR2 interactions) are shown as balls and sticks. HR2 chains are shown as green ribbons and HR1 chains as blue and red ribbons. The red region of HR1 corresponds to the sequences protected from proteinase K digestion. The entire stretch of HR2 along with 12 additional amino acids at the N-terminus not shown in the model is protected from proteinase K digestion.

has been proposed to induce a conformational change of SV5 F (66, 67). This change is followed by the release of the

fusion peptide from the F protein and its insertion into the host cell membrane, leading to a further change in the conformation of F. All these events bring the heptad repeats (far apart in the sequence) together, an event which brings the viral envelope and the host cell membrane into proximity for fusion. The structural similarities among heptad repeat complexes of F proteins of SV5, RSV, NDV, and PPRV described here therefore suggest a common fusion mechanism among these paramyxoviruses.

Although there are similarities in the fusion core complex among various enveloped viruses, recent studies on the crystal structure of the entire F protein of NDV suggest that the orientation of HR1 with respect to the viral envelope is the opposite of that of influenza virus (25, 68). Further, the presence of another internal fusion peptide in F proteins of some viruses and its direct role in the fusion process suggest a new model for paramyxovirus-induced membrane fusion (3, 69, 70). Therefore, further studies on F protein-mediated fusion processes among various paramyxoviruses are required to obtain more insights into the fusion mechanism.

## REFERENCES

- Seth, S., and Shaila, M. S. (2001) The fusion protein of Peste des petits ruminants virus mediates biological fusion in the absence of hemagglutinin-neuraminidase protein, *Virology* 289, 86–94.
- Paterson, R. G., Hiebert, S. W., and Lamb, R. A. (1985) Expression at the cell surface of biologically active fusion and hemagglutinin-neuraminidase proteins of the paramyxovirus simian virus 5 from cloned cDNA, *Proc. Natl. Acad. Sci. U.S.A.* 82, 7520–7524.
- Ghosh, J. K., Peisajovich, S. G., and Shai, Y. (2000) Sendai virus internal fusion peptide: structural and functional characterization and a plausible mode of viral entry inhibition, *Biochemistry* 39, 11581–11592.
- Aroeti, B., Jovin, T. M., and Henis, Y. I. (1990) Rotational mobility of Sendai virus glycoproteins in membranes of fused human erythrocytes and in the envelopes of cell-bound virions, *Biochemistry* 29, 9119–9125.
- Sakai, Y., and Shibuta, H. (1989) Syncytium formation by recombinant vaccinia viruses carrying bovine parainfluenza 3 virus envelope protein genes, *J. Virol.* 63, 3661–3668.
- Ebata, S. N., Cote, M. J., Kang, C. Y., and Dimock, K. (1991) The fusion and hemagglutinin-neuraminidase glycoproteins of human parainfluenza virus 3 are both required for fusion, *Virology* 183, 437–441.
- Morrison, T., McQuain, C., and McGinnes, L. (1991) Complementation between avirulent Newcastle disease virus and a fusion protein gene expressed from a retrovirus vector: requirements for membrane fusion, *J. Virol.* 65, 813–822.
- Taylor, J., Pincus, S., Tartaglia, J., Richardson, C., Alkhatib, G., Briedis, D., Appel, M., Norton, E., and Paoletti, E. (1991) Vaccinia virus recombinants expressing either the measles virus fusion or hemagglutinin glycoprotein protect dogs against canine distemper virus challenge, *J. Virol.* 65, 4263–4274.
- Wild, T. F., Malvoisin, E., and Buckland, R. (1991) Measles virus: both the haemagglutinin and fusion glycoproteins are required for fusion, *J. Gen. Virol.* 72, 439–442.
- Horvath, C. M., Paterson, R. G., Shaughnessy, M. A., Wood, R., and Lamb, R. A. (1992) Biological activity of paramyxovirus fusion proteins: factors influencing formation of syncytia, *J. Virol.* 66, 4564–4569.
- Hu, X. L., Ray, R., and Compans, R. W. (1992) Functional interactions between the fusion protein and hemagglutinin-neuraminidase of human parainfluenza viruses, *J. Virol.* 66, 1528–1534 [5176 (erratum)].
- Cattaneo, R., and Rose, J. K. (1993) Cell fusion by the envelope glycoproteins of persistent measles viruses which caused lethal human brain disease, *J. Virol.* 67, 1493–1502.
- Yao, Q., Hu, X., and Compans, R. W. (1997) Association of the parainfluenza virus fusion and hemagglutinin-neuraminidase glycoproteins on cell surfaces, *J. Virol.* 71, 650–656.
- Lamb, R. A. (1993) Paramyxovirus fusion: a hypothesis for changes, *Virology* 197, 1–11.

15. Homma, M., and Ohuchi, M. (1973) Trypsin action on the growth of Sendai virus in tissue culture cells. III. Structural differences of Sendai viruses grown in eggs and tissue culture cells, *J. Virol.* *12*, 1457–1465.
16. Scheid, A., and Chopin, P. W. (1974) Identification of biological activities of paramyxovirus glycoproteins. Activation of cell fusion, hemolysis, and infectivity of proteolytic cleavage of an inactive precursor protein of Sendai virus, *Virology* *57*, 475–490.
17. Morrison, T., Ward, L., and Semerjian, A. (1985) Intracellular processing of the Newcastle disease virus fusion glycoprotein, *J. Virol.* *53*, 851–857.
18. Klenk, H. D., and Garten, W. (1994) Host cell proteases controlling virus pathogenicity, *Trends Microbiol.* *2*, 39–43.
19. Novick, S. L., and Hoekstra, D. (1988) Membrane penetration of Sendai virus glycoproteins during the early stage of fusion with liposomes as determined by hydrophobic affinity labeling, *Proc. Natl. Acad. Sci. U.S.A.* *85*, 7433–7437.
20. Horvath, C. M., and Lamb, R. A. (1992) Studies on the fusion peptide of a paramyxovirus fusion glycoprotein: roles of conserved residues in cell fusion, *J. Virol.* *66*, 2443–2445.
21. Buckland, R., Malvoisin, E., Beauverger, P., and Wild, F. (1992) A leucine zipper structure present in the measles virus fusion protein is not required for its tetramerization but is essential for fusion, *J. Gen. Virol.* *73*, 1703–1707.
22. Sergel-Germano, T., McQuain, C., and Morrison, T. (1994) Mutations in the fusion peptide and heptad repeat regions of the Newcastle disease virus fusion protein block fusion, *J. Virol.* *68*, 7654–7658.
23. Rapaport, D., and Shai, Y. (1994) Interaction of fluorescently labeled analogues of the amino-terminal fusion peptide of Sendai virus with phospholipid membranes, *J. Biol. Chem.* *269*, 15124–15131.
24. Reitter, J. N., Sergel, T., and Morrison, T. G. (1995) Mutational analysis of the leucine zipper motif in the Newcastle disease virus fusion protein, *J. Virol.* *69*, 5995–6004.
25. Dutch, R. E., Jardetzky, T. S., and Lamb, R. A. (2000) Virus Membrane Fusion Proteins: Biological Machines that Undergo a Metamorphosis, *Biosci. Rep.* *20*, 597–612.
26. Wild, C., Oas, T., McDanal, C., Bolognesi, D., and Matthews, T. (1992) A synthetic peptide inhibitor of human immunodeficiency virus replication: correlation between solution structure and viral inhibition, *Proc. Natl. Acad. Sci. U.S.A.* *89*, 10537–10541.
27. Wild, T. F., Fayolle, J., Beauverger, P., and Buckland, R. (1994) Measles virus fusion: role of the cysteine rich region of the fusion glycoprotein, *J. Virol.* *68*, 7546–7548.
28. Rapaport, D., Ovadia, M., and Shai, Y. (1995) A synthetic peptide corresponding to a conserved heptad repeat domain is a potent inhibitor of Sendai virus-cell fusion: an emerging similarity with functional domains of other viruses, *EMBO J.* *14*, 5524–5531.
29. Lambert, D. M., Barney, S., Lambert, A. L., Guthrie, K., Medinas, R., Davis, D. E., Bucy, T., Erickson, J., Merutka, G., and Petteaway, S. R. J. (1996) Peptides from conserved regions of paramyxovirus fusion (F) proteins are potent inhibitors of viral fusion, *Proc. Natl. Acad. Sci. U.S.A.* *93*, 2186–2191.
30. Yao, Q., and Compans, R. W. (1996) Peptides corresponding to the heptad repeat sequence of human parainfluenza virus fusion protein are potent inhibitors of virus infection, *Virology* *223*, 103–112.
31. Young, J. K., Hicks, R. P., Wright, G. E., and Morrison, T. G. (1997) Analysis of a peptide inhibitor of paramyxovirus (NDV) fusion using biological assays, NMR, and molecular modeling, *Virology* *238*, 291–304.
32. Joshi, S. B., Dutch, R. E., and Lamb, R. A. (1998) A core trimer of the paramyxovirus fusion protein: parallels to influenza virus hemagglutinin and HIV-1 gp41, *Virology* *248*, 20–34.
33. Ben-Efrain, I., Kliger, Y., Harmesh, C., and Shai, Y. (1999) Membrane-induced step in the activation of Sendai virus fusion protein, *J. Mol. Biol.* *285*, 609–625.
34. Ghosh, J. K., Ovadia, M., and Shai, Y. (1997) A Leucine Zipper Motif in the Ectodomain of Sendai Virus Fusion Protein Assembles in Solution and in Membranes and Specifically Binds Biologically-Active Peptides and The Virus, *Biochemistry* *36*, 15451–15462.
35. Hernandez, L. D., Hoffman, L. R., Wolfsberg, T. G., and White, J. M. (1996) Virus-cell and cell-cell fusion, *Annu. Rev. Cell Dev. Biol.* *12*, 627–661.
36. Eckert, D. M., Malshkevich, V. N., Hong, L. H., Carr, P. A., and Kim, P. S. (1999) Inhibiting HIV-1 entry: discovery of D-peptide inhibitors that target the gp41 coiled-coil pocket, *Cell* *99*, 103–115.
37. Ferrer, M., Kapoor, T. M., Strassmaier, T., Weissenhorn, W., Skehel, J. J., Oprian, D., Schreiber, S. L., Wiley, D. C., and Harrison, S. C. (1999) Selection of gp41-mediated HIV-1 cell entry inhibitors from biased combinatorial libraries of non-natural binding elements, *Nat. Struct. Biol.* *6*, 953–960.
38. Lawless-Delmedico, M. K., Sista, P., Sen, R., Moore, N. C., Antczak, J. B., White, J. M., Greene, R. J., Leanza, K. C., Matthews, T. J., and Lambert, D. M. (2000) Heptad-repeat regions of respiratory syncytial virus F1 protein form a six-membered coiled-coil complex, *Biochemistry* *39*, 11684–11695.
39. Baker, K. A., Dutch, R. E., Lamb, R. A., and Jardetzky, T. S. (1999) Structural basis for paramyxovirus-mediated membrane fusion, *Mol. Cell* *3*, 309–319.
40. Miroux, B., and Walker, J. E. (1996) Over-production of proteins in *Escherichia coli*: mutant hosts that allow synthesis of some membrane proteins and globular proteins at high levels, *J. Mol. Biol.* *260*, 289–298.
41. Meyer, G., and Diallo, A. (1995) The nucleotide sequence of the fusion protein gene of the peste des petits ruminants virus: the long untranslated region in the 5'-end of the F-protein gene of morbilliviruses seems to be specific to each virus, *Virus Res.* *37*, 23–35.
42. Reed, L. J., and Muench, H. (1938) *Am. J. Hyg.* *37*, 493.
43. Greenfield, N., and Fasman, G. D. (1969) Computed circular dichroism spectra for the evaluation of protein conformation, *Biochemistry* *8*, 4108–4116.
44. Wu, C. S. C., Ikeda, K., and Yang, J. T. (1981) Ordered conformation of polypeptides and proteins in acidic dodecyl sulfate solution, *Biochemistry* *20*, 566–570.
45. Chen, Y. H., Yang, J. T., and Chau, K. H. (1974) Determination of the helix and beta form of proteins in aqueous solution by circular dichroism, *Biochemistry* *13*, 3350–3359.
46. Rost, B., and Sander, C. (1993) Prediction of protein secondary structure at better than 70% accuracy, *J. Mol. Biol.* *232*, 584–599.
47. Rost, B. (1996) PHD: predicting one-dimensional protein structure by profile-based neural networks, *Methods Enzymol.* *266*, 525–539.
48. Wolf, P., Kim, P. S., and Berger, B. (1997) MultiCoil: A Program for Predicting Two- and Three-Stranded Coiled Coils, *Protein Sci.* *6*, 1179–1189.
49. Thompson, J. D., Higgins, D. G., and Gibson, T. J. (1994) CLUSTALW: improving the sensitivity of progressive multiple sequence alignment through sequence weighting, position-specific gap penalties and weight matrix choice, *Nucleic Acids Res.* *22*, 4673–4680.
50. Sutcliffe, M. J., Haneef, I., Carney, D., and Blundell, T. L. (1987) Knowledge based modeling of homologous proteins, Part I: Three-dimensional frameworks derived from the simultaneous superposition of multiple structures, *Protein Eng.* *1*, 377–384.
51. Sutcliffe, M. J., Hayes, F. R., and Blundell, T. L. (1987) Knowledge based modeling of homologous proteins, Part II: Rules for the conformations of substituted sidechains, *Protein Eng.* *1*, 385–392.
52. Srinivasan, N., and Blundell, T. L. (1993) An evaluation of the performance of an automated procedure for comparative modeling of protein tertiary structure, *Protein Eng.* *6*, 501–512.
53. Weiner, S. I., Kollman, P. A., Case, D. A., Singh, U. C., Ghio, C., Alagona, G., Profeta, S., and Weiner, P. (1984) A new force field for molecular mechanical simulation of nucleic acids and proteins, *J. Am. Chem. Soc.* *106*, 765–784.
54. Evans, S. V. (1993) Hardware lighted three-dimensional solid model representations of macromolecules, *J. Mol. Graphics* *11*, 134–138.
55. Citovsky, V., Yanai, P., and Loyter, A. (1986) The use of circular dichroism to study conformational changes induced in Sendai virus envelope glycoproteins. A correlation with the viral fusogenic activity, *J. Biol. Chem.* *261*, 2235–2239.
56. Wild, T. F., and Buckland, R. (1997) Inhibition of measles virus infection and fusion with peptides corresponding to the leucine zipper region of the fusion protein, *J. Gen. Virol.* *78*, 107–111.
57. Yu, M., Wang, E., Liu, Y., Cao, D., Jin, N., Zhang, C. W., Bartlam, M., Rao, Z., Tien, P., and Gao, G. F. (2002) Six-helix bundle

- assembly and characterization of heptad repeat regions from the F protein of Newcastle disease virus, *J. Gen. Virol.* 83, 623–629.
58. Ghosh, J. K., Peisajovich, S. G., Ovadia, M., and Shai, Y. (1998) Structure–function study of a heptad repeat positioned near the transmembrane domain of Sendai virus fusion protein which blocks virus-cell fusion, *J. Biol. Chem.* 273, 27182–27190.
59. Matthews, J. M., Young, T. F., Tucker, S. P., and Mackay, J. P. (2000) The core of the respiratory syncytial virus fusion protein is a trimeric coiled coil, *J. Virol.* 74, 5911–5920.
60. Dutch, R. E., Leser, G. P., and Lamb, R. A. (1999) Paramyxovirus fusion protein: characterization of the core trimer, a rod shaped complex with helices in anti-parallel orientation, *Virology* 254, 147–159.
61. Zhao, X., Singh, M., Malashkevich, V. N., and Kim, P. S. (2000) Structural characterization of the human respiratory syncytial virus fusion protein core, *Proc. Natl. Acad. Sci. U.S.A.* 97, 14172–14177.
62. Wilson, I. A., Skehel, J. J., and Wiley, D. C. (1981) Structure of the haemagglutinin membrane glycoprotein of influenza virus at 3 Å resolution, *Nature* 289, 366–375.
63. Bullough, P. A., Hughson, F. M., Skehel, J. J., and Wiley, D. C. (1994) Structure of influenza haemagglutinin at the pH of membrane fusion, *Nature* 371, 37–43.
64. Chen, J., Skehel, J. J., and Wiley, D. C. (1999) N- and C-terminal residues combine in the fusion pH influenza hemagglutinin HA2 subunit to form an N cap that terminates the triple-stranded coiled coil, *Proc. Natl. Acad. Sci. U.S.A.* 96, 8967–8972.
65. Durrer, P., Galli, C., Hoenke, S., Corti, C., Gluck, R., Vorherr, T., and Brunner, J. (1996) H<sup>+</sup>-induced membrane insertion of influenza virus hemagglutinin involves the HA2 amino-terminal fusion peptide but not the coiled coil region, *J. Biol. Chem.* 271, 13417–13421.
66. Paterson, R. G., Russell, C. J., and Lamb, R. A. (2000) Fusion protein of the paramyxovirus SV5: destabilizing and stabilizing mutants of fusion activation, *Virology* 242, 17–30.
67. Russell, C. J., Jardetzky, T. S., and Lamb, R. A. (2001) Membrane fusion machines of paramyxoviruses: capture of intermediates of fusion, *EMBO J.* 20, 4024–4034.
68. Chen, L., Gorman, J. J., McKimm-Breschkin, J., Lawrence, L. J., Tulloch, P. A., Smith, B. J., Colman, P. M., and Lawrence, M. C. (2001) The structure of the fusion glycoprotein of Newcastle disease virus suggests a novel paradigm for the molecular mechanism of membrane fusion, *Structure* 9, 255–266.
69. Samuel, O., and Shai, Y. (2001) Participation of two fusion peptides in measles virus-induced membrane fusion: emerging similarity with other Paramyxovirus-mediated membrane fusion, *Biochemistry* 40, 1340–1349.
70. Peisajovich, S. G., and Shai, Y. (2002) New insights into the mechanism of virus-induced membrane fusion, *Trends Biochem. Sci.* 27, 183–190.

BI026858D